

Three Dimensionally Ordered Microstructure of Polycrystalline TiO₂ Ceramics with Micro/meso Porosity

Myung Chul Chang[†]

Department of Materials Science and Engineering, Kunsan National University, Gunsan 51450, Korea

(Received January 6, 2016; Revised February 3, February 13, 2016; Accepted February 15, 2016)

ABSTRACT

In order to make a highly ordered three-dimensional porous structure of titania ceramics, porogen beads of PS [Polystyrene] and PMMA [poly(methylmetacrylate)] were prepared by emulsion polymerization using styrene monomer and methyl methacrylate monomer, respectively. The uniform beads of PS or PMMA latex were closely packed by centrifugation as a porogen template for the infiltration of titanium butoxide solution. The mixed compound of PS or PMMA with titanium butoxide was dried and the dry compacts were calcined at 450°C - 750°C according to the firing schedule to prepare micro- and meso- structures of polycrystalline titania with monodispersed porosity. Inorganic frameworks composed of TiO₂ were formed and showed a three Dimensionally Ordered Microstructure [3DOM] of TiO₂ ceramics. The pulverized particles of the TiO₂ ceramic skeleton were characterized using XRD analysis. A monodispersed crystalline micro-structure with micro/meso porosity was observed by FE-SEM with EDX analysis. The 3DOM TiO₂ skeleton showed opalescent color tuning according to the direction of light.

Key words : Honeycomb skeleton, Monodispersed nano-beads, Titanium butoxide, Monodisperse TiO₂, Uniform porosity

1. Introduction

TiO₂ has been widely investigated and used because it is nontoxic, easy to make, inexpensive, and chemically stable. Synthesis of highly crystalline titania nanoparticles with controlled crystal structure, morphology, and size has been a very active field in materials chemistry.¹⁻³⁾ We have focused on the microstructural development of polycrystalline oxide ceramics having uniform grains and monodispersed pores.⁴⁻⁶⁾ On a microstructural basis of catalytic oxide ceramics, a three dimensionally ordered microstructure [3DOM] of polycrystalline ceramics has been studied and the preparation technology has been widely developed according to the application field.¹⁻⁶⁾

In this study, a 3DOM structure was developed using monodispersed titanium oxide powders and porogen beads, which were synthesized using the published methods.^{7,8)} A 3DOM titania network was prepared by colloidal crystal templating⁹⁻²⁴⁾ using Ti-butoxide; the template was beads of PMMA [poly(methylmetacrylate)] or PS [Polystyrene].^{8,14-19)}

2. Experimental Procedure

2.1 Preparation of porogen beads of PS

For the preparation of PS,¹⁴⁻¹⁷⁾ we used the micro-emulsion [PS] process and surfactant-free [SFree-PS] emulsion

process.^{13,22)} The emulsion polymerization starts with an emulsion incorporating water, monomer, and surfactants. In order to make an oil-in-water emulsion, droplets of monomer (the oil) are emulsified (with surfactants) in a continuous phase of water. A conventional emulsion system with styrene 7.84 wt %, SDS 1.96 wt %, water 90.20 wt %, and KPS 3.60 mM is polymerized at 70°C.

2.1.1 Micro-emulsion process

The micro-emulsion^{15-17,20)} was prepared by drop-wise addition of styrene into the SDS/1-pentanol/H₂O system at room temperature; resulting mixture was polymerized in a 3-necked flask under a pure nitrogen atmosphere to complete conversion at 70°C for the former. The recipe was as follows (wt %): styrene 1.37, SDS 10.10, 1-pentanol 1.24, and water 87.29. The concentration of KPS was 0.38 mM.

2.1.2 Surfactant-free emulsion process

Surfactant-free mono-disperse PS latex spheres were synthesized using an emulsifier-free emulsion polymerization technique.^{13,22)} All water was distilled and deionized to a resistivity of at least 17.6 MΩ-cm. Styrene monomer (210 mL) was washed in a separatory funnel four times with 200 mL of 0.1 M NaOH, then four times with 200 mL of water. A five-necked, 3000 mL round-bottomed flask was filled with 1700 mL of water and heated to 70°C before 200 mL of the washed styrene was added. An electric motor driving a glass stirring rod with a Teflon wedge was attached to the flask, in which there were a thermometer, a condenser, a pipet through which house nitrogen was bubbled to deaerate the mixture, and a stopper for the addition of reactants.

[†]Corresponding author: Myung Chul Chang
E-mail: mcchang@kunsan.ac.kr
Tel: +82-63-469-4735 Fax: +82-63-462-6982

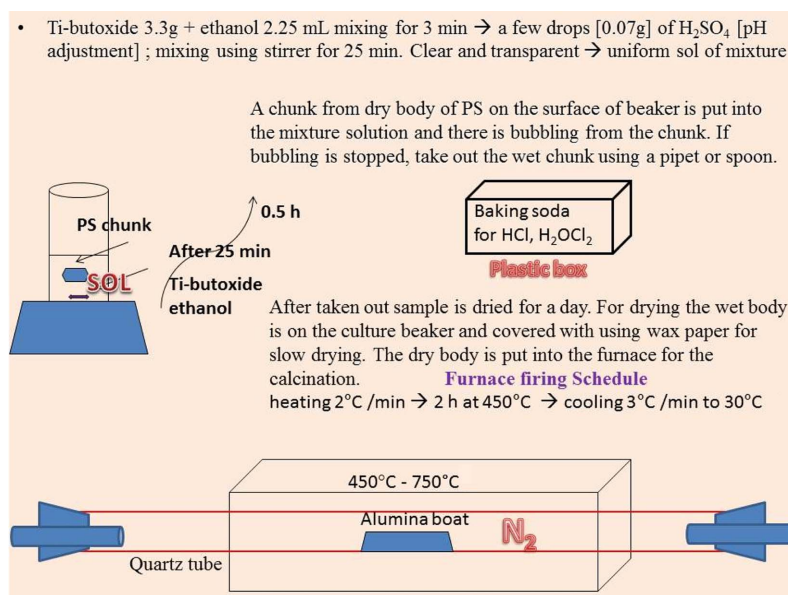


Fig. 1. Preparation process of 3DOM skeleton using Ti-butoxide with PMMA beads or PS beads.

In a separate 160-mL polyethylene bottle, 0.663 g of potassium persulfate initiator, KPS, was added to 100 mL of water, and the solution was then heated to 70°C. The water and styrene solution was reheated to 70°C and the initiator was added. To facilitate later removal of the latex spheres from the macro-porous product, no cross-linking agent was added. The temperature was kept at 70°C while the solution was stirred at 245 or 360 rpm for 28 h. The resulting latex spheres were filtered through glass wool to remove any large agglomerates. The latex spheres remained suspended in their mother liquor until needed. Before use, the spheres were centrifuged at 900 - 1000 rpm for 12 to 24 h, then allowed to air-dry.

2.2 Preparation of porogen beads of PMMA

PMMA spheres of uniform diameter were prepared by surfactant-free emulsion polymerization, as reported.^{8,14,21} For the preparation process of PMMA latex beads, the chemicals were methyl methacrylate monomer [M55909, Sigma Aldrich, USA] and granular 2,2'-Azobis(2-methylpropanamide) dihydrochloride, an AMPD initiator [M440914, Sigma Aldrich, USA]. In order to make 0.5-1.5 g of macroporous material, we used 10 g of PMMA. Polymerization was initiated with the AMPD initiator. The colloidal suspension was centrifuged at 1500 rpm for 24 h; water was decanted and the solid was allowed to dry for 3 days to sediment the spheres. The five neck round-bottom flask [Sigma Aldrich] was clearly cleaned before the start of the polymer reaction of PMMA. The capacity of the five-neck flask was 3,000 mL with center Joint: ST/NS 24/40. The cleaning of PMMA chunks was performed using acetone, tetrahydrofuran [THF] [Sigma Aldrich], a flow meter, and baking soda, this last of which was used to remove Cl gas (Fig. 1(a)).

2.3 Preparation of 3DOM skeleton

Cleaning of the 5 neck reactor for the PMMA template was performed in order to obtain good cakes. The dry cake chunk material, a mixture of unreacted polymer of PMMA and spheres, was softened using acetone and/or THF; the wet chunk material was cut and taken out using a spoon or pipet. This serious cleaning took 1.5 h; later, the utilized solvent was reused. For the formation of the 3DOM structure of the TiO₂ skeleton, we used PMMA beads as one of the porogen materials. The dry body of the centrifuged PMMA was crushed; a three gram PMMA block sample was obtained as wet-like lumps.

Surfactant-free PS or PMMA latex spheres were synthesized using an emulsifier-free emulsion polymerization technique.^{8,13,14,21,22} The diameters of the mono-disperse PMMA or PS latex spheres were approximately 500 nm or 750 nm, respectively. We used pieces of broken polymer pallets in the flask inner surface to prepare the colloidal crystal template of the PS spheres in the centrifuge at 1000 rpm. The diameters of the pieces of broken polymer pellets that were taken out as types of latex chunks were between 0.5 cm and 1.5 cm after the polymerization in the five neck flask of the PS template. Dry bodies of the centrifuged PS were crushed and came to look like wet lumps of PS chunks, as shown in the left picture of Fig. 1.

For the synthesis of 3DOM TiO₂, 3.3 g of titanium butoxide [Ti(CH₂OH)₄, Sigma Aldrich] was mixed with 2.25 mL of ethanol and stirred for 3 minutes, as shown in Fig. 1. A few drops of 0.07 g H₂SO₄ were added for pH adjustment. The mixture solution was stirred for 25 min. The solution started to become a transparent and uniform sol. As can be seen in Fig. 1, a chunk from the dry body of the PMMA or PS on the surface of the beaker was put into the mixture solution. We were able to observe bubbling from the chunk.

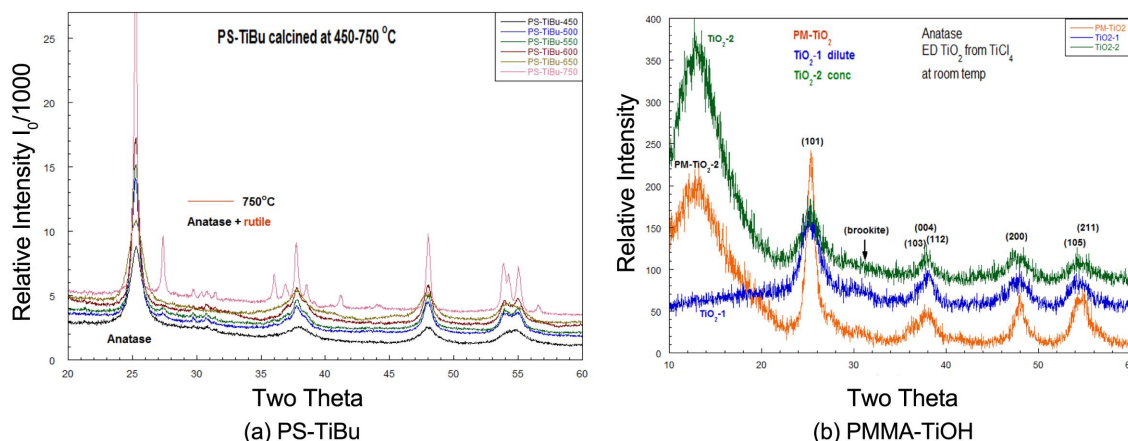


Fig. 2. XRD spectra for TiO₂ powder samples, in which 3DOM structure was prepared using porogen spheres of PS and PMMA. (a) Heat-treated mixture of PS with Ti-butoxide, (b) dry mixture of PMMA with nanoparticles of anatase TiO₂.

If the bubbling stopped, the wet chunk was taken out and the sample was dried for a day. For drying, the wet body was put on the culture beaker and covered with wax paper for slow drying. For the calcination, the cakes of dry powder were poured into an alumina crucible and put into a furnace, as shown in the last part of Fig. 1. According to the firing schedule, the cakes were calcined in a temperature range of 450°C to 750°C for two hours; they were then cooled to 30°C. During the calcination process, N₂ gas was passed through baking soda in a plastic box and then was supplied into the quartz tube in the furnace. The amount of flowing N₂ gas was controlled by counting the number of gas bubbles in the attached flask.

2.4 Characterization

XRD [Bruker, M18XCE] was used for the characterization of the TiO₂ ceramic skeleton after the firing process. The sample body was pulverized into TiO₂ powder for the XRD measurement using a Cu target. The microstructure of the sintered TiO₂ body was investigated using FE-SEM [Hitachi S4800, Japan].

3. Results and Discussion

The critical factor in optimizing the optical properties of titania materials is the ability to control the fine structure of the boundary layer walls of the 3DOM skeleton.^{8,12-14,20-29} The titania walls are composed of condensed nanocrystals whose sizes influence the optical response of the material. For example, well-ordered 3DOM titania with 30 nm wall grains appears white, while a material with 2 nm grains exhibits brilliant colors like opal.²⁴⁻²⁹ One aspect of our research involves optimizing nano-grain sizes and phases by controlling the precursor chemistry, template–precursor interfacial interactions, and processing conditions. Construction of three dimensional structures is difficult and expensive. Chemical routes involve the use of colloidal crystal templates to form 3DOM polycrystalline structures.

Monodisperse spheres of PMMA or PS are closely packed into ordered arrays and infiltrated with a fluid, which is solidified. After removal of the template, a solid skeleton is obtained around the ordered array of voids where the original spheres were located.

Figure 2 shows results of the XRD analysis of the TiO₂ ceramic skeleton (a) and TiO₂ powders (b). In Fig. 2(a), it can be seen that PS beads were impregnated with the Ti-butoxide solution and that the 3DOM structure was developed after the drying and calcination. The samples were calcined at 450°C, 500°C, 550°C, 600°C, 650°C, and 750°C. PS-TiBu-450 sample indicates that the sample was mixed with Ti-butoxide and PS beads and fired at 450°C for 2 h. In Fig. 2(b), it can be seen that TiO₂ nano-crystalline particles were prepared by precipitation process using aqueous TiCl₄.^{8,30,31} In order to make the PM-TiO₂-2 sample, PMMA beads were mixed with a wet paste of TiOH nano-particles prepared by electrodialysis [ED] process^{7,8} using aqueous TiCl₄; next, the wet mixture was dried at room temperature. As reported,⁸ TiO₂-1 and TiO₂-2 were prepared at low concentration and higher concentration, respectively, in solution-precipitation reactions using TiCl₄ precursor at room temperature. In the PM-TiO₂-2 sample, PMMA beads were impregnated into the TiOH paste, which was precipitated by using a higher concentration TiCl₄ aqueous solution.

In the XRD data, it can be seen that PM-TiO₂-2, shown in Fig. 2(b), has anatase crystal phase spectra. In Fig. 2(a) PS-TiBu-450 shows a tetragonal crystal phase; the crystallinity increases with temperature increase. At 750°C, the rutile phase clearly appears with the anatase crystals. These crystal phase results can be related with the microstructural development of the TiO₂ layers, as shown in Fig. 3 - Fig. 6.

3.1 Preparation of homogeneous beads of PS

After Dynosphere[®] was first fabricated at the University of Michigan (under the support of Dow Chemical), PS latex has been typically been composed of monodispersed micro/nano-particles. In this emulsion-free polymerization pro-

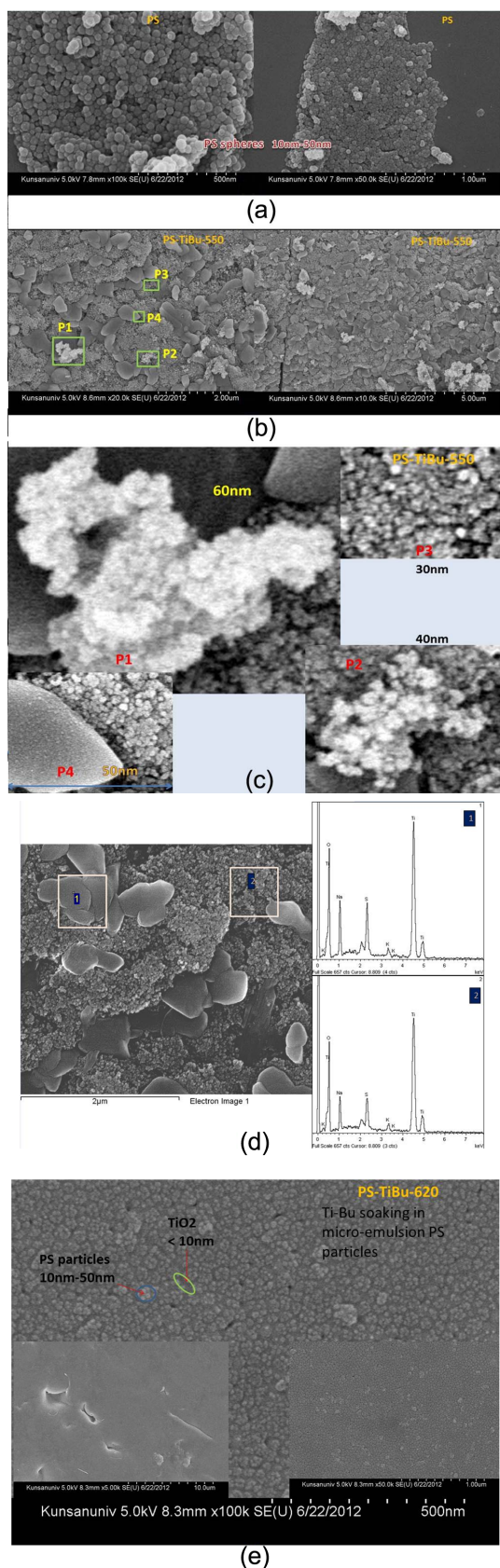


Fig. 3. FE-SEM micrographs for (a) the PS at room temperature, (b) PS-TiBu-550 and (e) PS-TiBu-620. (c) Enlarged pictures for the positions of 1, 2, 3, and 4 in (b) and (d) EDX patterns for region 1 and region 2.

cess, the diameters of the PS beads are known to be between 100 nm and 600 nm. Using emulsion polymerization, we can obtain nano-beads with diameters above 50 nm; in micro-emulsion polymerization, nano-beads with diameters below 50 nm are obtained. For the semi-continuous micro-emulsion polymerization of styrene, we used SDS [Sodium dodecylsulfate] emulsifier [MICOLIN, Miwon]. Additionally we prepared surfactant-free PS beads. From the FE-SEM microstructure shown in Fig. 3(a), it can be seen that the diameters of the PS beads is between 10 nm and 50 nm. Fig. 4(a) shows the microstructure of SFree-PS-TiBu; in this sample, the PS beads were prepared by surfactant-free polymerization; the diameter of the mono-disperse PS beads is estimated to be ~ 700 nm.

3.2 Preparation of homogeneous beads of PMMA

PMMA latex spheres with diameters of 500 nm were obtained, as shown in Fig. 4(b). The synthesized raw compounds were stirred and centrifuged in a five neck flask reactor at 1000 rpm. As a colloidal crystal template, pellets were formed from the polymer. Pieces of broken polymer pellets on the surface of flask were taken out; the pellet sizes were from roughly 0.5 cm to 1.5 cm. PMMA is less toxic than polystyrene. For the preparation of the template cakes, the mixture of unreacted PMMA and spheres was softened using acetone and/or THF. Using a spoon, the chunk was pulled out and cut. This case was serious and took 1.5 hrs. The obtained PMMA powder aggregates can be ground simply using a finger to push the aggregates between the weighing covers.

3.3 Three dimensionally ordered microstructure of anatase ceramics

Figure 3(b) shows the 3DOM structure of the PS-TiBu-550 sample calcined at 550°C. In this sample, the PS beads were prepared through micro-emulsion polymerization; the sizes were between 10 nm and 50 nm, as can be seen in Fig. 3(a). In the 3DOM structure of the PS-TiBu-550 sample, shown in Fig. 3(b), we can observe the crystal growth of TiO₂ particles during the firing process. Fig. 3(c) provides enlarged pictures of the rectangular positions of P1, P2, P3, and P4 in the left micrograph of Fig. 3(b). Several-nanometer particles of TiO₂ were grown and agglomerated to several tens-of-nanometer granules; the abnormal grain growth turned into a several-hundred-nm single crystal (P4). Fig. 3(d) shows the results of an EDX taken for a single crystal region (1) and for the agglomerated particle region (2). X-ray spectra analysis shows similar patterns in the two regions, indicating that there are only slight differences in the composition and intensity of the anatase TiO₂ phase. Considering these results, it seems that condensation via solid state reaction among TiO₂ nano-particles occurred at 550°C. During the firing process, several-nm pore channels were infiltrated with TiO₂ nano-particles by capillary pressure; the 3DOM architecture became dense through the solid-state condensation of TiO₂ nano-particles. Fig. 3(e) shows

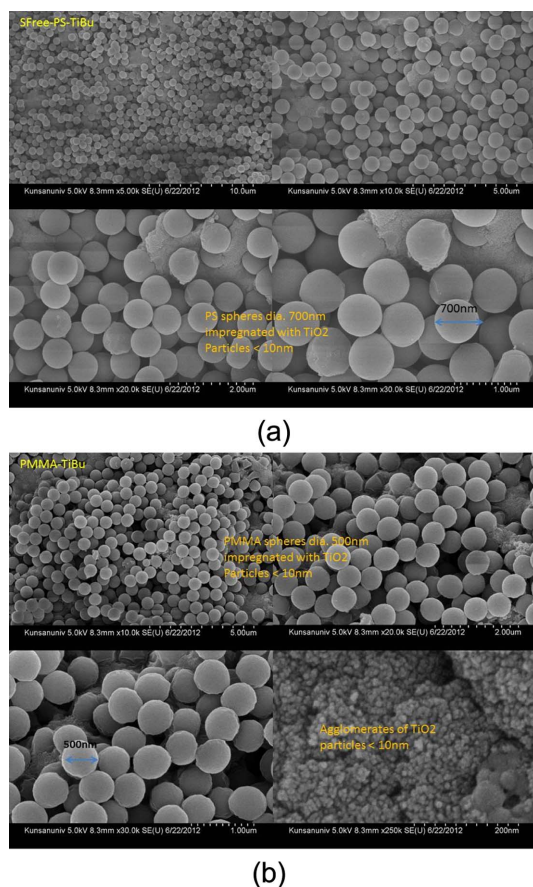


Fig. 4. FE-SEM micrographs for (a) PS-TiBu at room temperature and (b) PMMA-TiBu at RT at room temperature. (a) PS beads were impregnated in Ti-butoxide solution. (b) PMMA beads were mixed with Ti-butoxide solution.

the 3DOM structure of the PS-TiBu-620 sample, for which PS was prepared using the micro-emulsion process and Ti-butoxide solution was infiltrated with the monodispersed PS particles. The dry mixture of Ti-butoxide and PS beads was calcined at 620°C. The particle size of TiO₂ is several nm and the diameter of the PS beads is in the range of 10 to 50 nm.

In Fig. 4(a), showing the 3DOM microstructure of the SFree-PS-TiBu, monodispersed PS beads with diameters of ~ 700 nm were impregnated in the Ti-butoxide ethanol solution and the resulting mixture was dried at room temperature. Fig. 4(b) shows the 3DOM microstructure of the PMMA-TiBu compound at room temperature. The size of the PMMA mono-spheres is ~ 500 nm; we can observe agglomerates of several-nm monospheres of TiO₂. In the experimental process, PMMA beads were impregnated in the Ti-butoxide ethanol solution. From the information presented in Fig. 4 and Fig. 5, it can be postulated that the uniform distribution of PMMA changes according to the volumetric mixing ratio of PMMA beads in the Ti-butoxide solution. During the FE-SEM observation, we were able to observe a uniform distribution, as shown in Fig. 5(b)(c)(d)(e). On the other hand, it was occasionally possible to observe

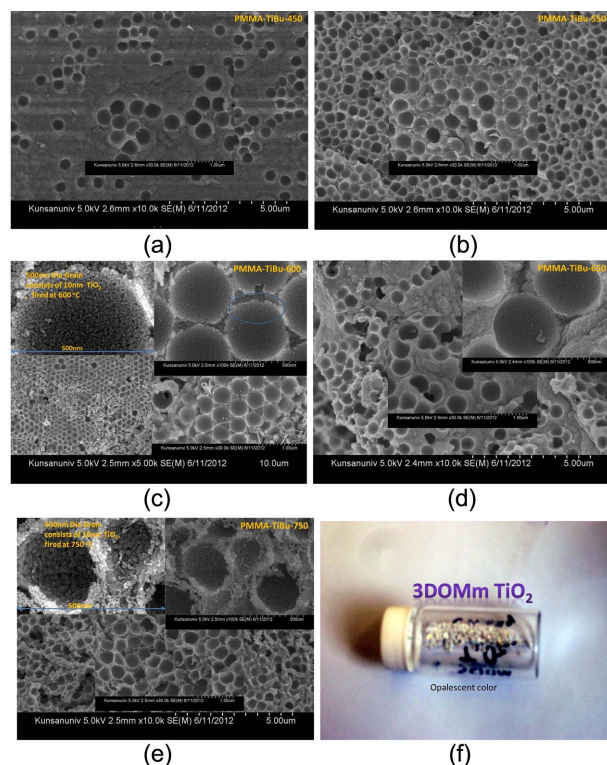


Fig. 5. FE-SEM 3DOM micrographs for PMMA-TiO₂ samples fired at 450°C, 550°C, 600°C, 650°C, and 750°C. (a) PMMA-TiBu-450, (b) PMMA-TiBu-550, (c) PMMA-TiBu-600, (d) PMMA-TiBu-650, and (e) PMMA-TiBu-750. (f) Opalescent view of 3DOM TiO₂ granules in air for PMMA-TiBu-750 sample, in which PMMA/Ti-butoxide mixture was fired at 750°C.

the non-uniform distribution that is seen in Fig. 5(a) in most of the samples. In order to obtain a uniform 3DOM bulk structure, the process should be more finely controlled. Fig. 5 shows the 3DOM structure of the PMMA-TiBu samples calcined at 450°C, 550°C, 600°C, 650°C, and 750°C for PMMA-TiBu-450, PMMA-TiBu-550, PMMA-TiBu-600, PMMA-TiBu-650, and PMMA-TiBu-750, respectively. In Fig. 5(f), the monodispersed TiO₂ granules show opalescent behavior²⁵⁻²⁹ according to the direction of light for the PMMA-TiBu-750 sample from Fig. 5(e). The boundary layer Ti-OH compound between the PMMA beads was calcined and formed into an agglomerate of TiO₂ granules and the 3DOMm structure of TiO₂. Monodispersed beads of PMMA or PS, shown in Fig. 4(a) (b), exhibit opalescent color emission according to the light direction, which is the typical behavior of mono-dispersed beads.^{8,24-29} The color emission varies with the dimensions of monodispersed beads and with the type of added solution, such as water, alcohol, or toluene. The 3DOM skeleton of the TiO₂ granules with several-nm pores was filled with the solvent; increasing the pore size or filling the pores with solvent resulted in an increase in the wavelength of light reflected by the photonic crystal.²⁸⁻³²

In Fig. 5(c), the pore size and the boundary wall thickness of PMMA-TiBu-600 were estimated to be ~ 500 nm and ~ 10 nm, respectively. In the PMMA/Ti-butoxide sample, PMMA was

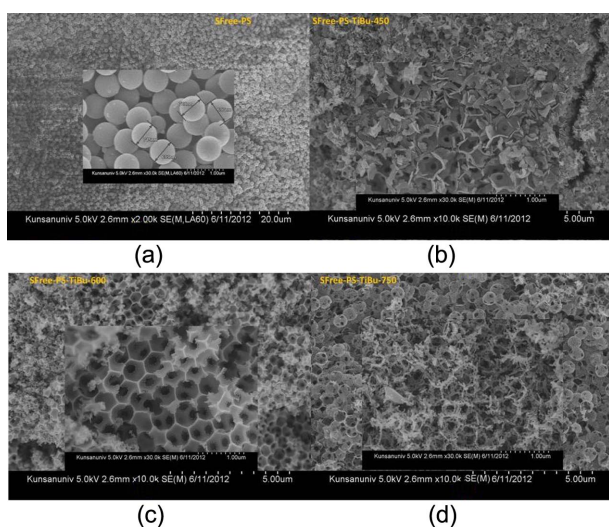


Fig. 6. FE-SEM 3DOM microstructure of PS beads at room temperature (a) and PS-TiBu samples, in which SFree-PS bead mixture with Ti-butoxide solution was calcined at (b) 450°C, (c) 600°C, and (d) 750°C for SFree-PS-TiBu-450, SFree-PS-TiBu-600, and SFree-PS-TiBu-750, respectively. The enlarged pictures in (c) and (d) show the grain growth of TiO₂ nano-particles at the boundary region of PS beads.

burned out through the slow firing schedule; the formed TiO₂ nano-powders were condensed at 450°C, as shown in Fig. 5. From the number of powder grains in the boundary, it is supposed that the diameter of TiO₂ powder at 450°C may be estimated to be ~5 nm. The dimensions of the pores formed by the burn-out of the 500 nm PMMA beads decreased to 480 nm and 270 nm for PMMA-TiBu-550 and PMMA-TiBu-750, respectively. During the initial stage of the firing process, the PMMA beads were burned out and TiO₂ nano-powders were formed through the evaporation of alcoholic groups attached to Ti-butoxide. With the increase of the firing temperature, the formed TiO₂ nanoparticles agglomerated to granules and the 3DOM skeleton of TiO₂ was built through the grain growth of TiO₂ granules in the boundary wall. In the sample calcined at 750°C, as shown in Fig. 5(e), crystallites of TiO₂ were condensed to larger grains in the network boundary region of the PMMA beads. In the magnified pictures, the boundary regions among the pores, which were formed by the burn-out of PMMA beads, became larger in the PMMA-TiBu-750 sample than these boundary regions did in the PMMA-TiBu-450 sample. The densification of the TiO₂ powders resulted in a larger grain size in the boundary region and in a smaller pore size of PMMA-TiBu-750.

Figure 6 shows the 3DOM structure of the Ti-butoxide mixture of PS; this mixture was prepared by surfactant-free polymerization, and the dry mixture was calcined at 450°C, 600°C, and 750°C for the samples of SFree-PS-TiBu-450, SFree-PS-TiBu-600, and SFree-PS-TiBu-750, respectively. Fig. 6(a) shows monodispersed uniform PS beads of 700 nm. The 3DOM structure developed with the firing temperature increase. In the high temperature samples shown in Fig. 6(c)

and Fig. 6(d), we can observe exaggerated grain growth at 600°C and 750°C, respectively. The grain growth induced a larger 3DOM wall structure for the higher temperature samples.

The next subject of research will be to determine the progress for controlling the morphologies of 3DOM materials at different length scales. To prepare periodic pore structures, void spaces between spheres in a colloidal crystal template are infiltrated by any type of fluid that can penetrate the template and can be converted into a solid. Removal of the template spheres leaves a solid skeleton that surrounds the air holes left in the original locations of the spheres.

4. Conclusions

A 3DOM structure of polycrystalline TiO₂ ceramics with micro- or meso- porosity was prepared using monodispersed beads of PMMA or PS, respectively. The mixed dry body of PMMA or PS beads with Ti-butoxide solution was slowly fired in a temperature range of 450°C to 750°C; resulting sample showed a mono-dispersed honeycomb skeleton of nano-sized crystalline titania particles. The formed 3DOM skeleton of TiO₂ granules in solvent showed opalescent color emission according to the light direction of the photonic crystals.

Acknowledgments

This research was supported by the general research support program of the National Research Foundation (NRF), funded by the Korean Government (2013R1A1A2A10058275).

REFERENCES

1. A. L. Linsebigler, G. Q. Lu, and J. T. Yates, "Photocatalysis on TiO₂ Surfaces: Principles, Mechanisms, and Selected Results," *Chem. Rev.*, **95** [3] 735-58 (1995).
2. B. O'Regan and M. Gratzel, "A Low-Cost, High-Efficiency Solar Cell based on Dye-Sensitized Colloidal TiO₂ Films," *Nature*, **353** 737-40 (1991).
3. H. Wang, Y. Wu, and B. Q. Xu, "Preparation and Characterization of Nanosized Anatase TiO₂ Cuboids for Photocatalysis," *Appl. Catal. B: Environmental*, **59** [3] 139-46 (2005).
4. H. Yan, F. B. Christophe, T. H. Brian, H. S. William, and A. Stein, "General Synthesis of Periodic Macroporous Solids by Templated Salt Precipitation and Chemical Conversion," *Chem. Mater.*, **12** [4] 1131-41 (2000).
5. A. Stein and R. C. Schroden, "Colloidal Crystal Templating of Three-Dimensionally Ordered Macroporous Solids: Materials for Photonics and Beyond," *Curr. Opin. Solid St. M.*, **5** [6] 553-64 (2001).
6. R. C. Schroden and A. Stein, "3D Ordered Macroporous Materials," pp. 465-93 in *Colloids and Colloid Assemblies: Synthesis, Modification, Organization and Utilization of Colloid Particles*, Ed. by F. Caruso, Wiley-VCH, Weinheim, 2003.

7. M. C. Chang, "Yttrium-Stabilized Zirconia Particles Prepared Using Electro-Dialysis of (Zr,Y)OCl₂ Aqueous Solution," *J. Korean Ceram. Soc.*, **51** [5] 466-71 (2014).
8. M. C. Chang, "Three Dimensionally Ordered Microstructure of Monodispersed Zirconia Particles with Micro/Meso Porosity," *J. Korean Ceram. Soc.*, **53** [1] 50-5 (2016).
9. K. M. Kulinowski, P. Jiang, H. Vaswani, and V. L. Colvin, "Porous Metals from Colloidal Templates," *Adv. Mater.* **12** [11] 833-38 (2000).
10. O. D. Velev and E. W. Kaler, "Structured Porous Materials via Colloidal Crystal Templating: from Inorganic Oxides to Metals," *Adv. Mater.*, **12** [7] 531-34 (2000).
11. O. D. Velev and A. M. Lenhoff, "Colloidal Crystals as Templates for Porous Materials," *Curr. Opin. Colloid In.*, **5** [1] 56-63 (2000).
12. A. Stein, "Sphere Templating Methods for Periodic Porous Solids," *Micropor. Mesopor. Mat.*, **44-45** 227-39 (2001).
13. B. T. Holland, C. F. Blanford, T. Do, and A. Stein, "Synthesis of Highly Ordered, Three-Dimensional, Macroporous Structures of Amorphous or Crystalline Inorganic Oxides, Phosphates, and Hybrid Composites," *Chem. Mater.*, **11** [3] 795-805 (1999).
14. Z. Wang and A. Stein, "Morphology Control of Carbon, Silica, and Carbon/Silica Nanocomposites: From 3D Ordered Macro-/Mesoporous Monoliths to Shaped Mesoporous Particles," *Chem. Mater.*, **20** [3] 1029-40 (2008).
15. N. T. Hunt, A. A. Jaye, A. Hellman, and S. R. Meech, "Ultrafast Dynamics of Styrene Micro-emulsions, Polystyrene Nano-latexes, and Structural Analogues of Polystyrene," *J. Phys. Chem. B*, **108** [1] 100-8 (2004).
16. X. J. Xu, P. Y. Chow, C. H. Quek, H. H. Hng, and L. M. Gan, "Nanoparticles of Polystyrene Latexes by Semi-continuous Micro-Emulsion Polymerization Using Mixed Surfactants," *J. Nanosci. Nanotechnol.*, **3** [3] 235-40 (2003).
17. W. Ming, J. Zhao, X. Lu, C. Wang, S. Fu, "Novel Characteristics of Polystyrene Microspheres Prepared by Micro-emulsion Polymerization," *Macromolecules*, **29** [24] 7678-82 (1996).
18. P. Jiang, J. F. Bertone, and V. L. Colvin, "A Lost-Wax Approach to Monodisperse Colloids and Their Crystals," *Science*, **291** 453-57 (2001).
19. P. Jiang, K. S. Hwang, D. M. Mittleman, J. F. Bertone, and V. L. Colvin, "Template-Directed Preparation of Macroporous Polymers with Oriented and Crystalline Arrays of Voids," *J. Am. Chem. Soc.*, **121** [50] 11630-37 (1999).
20. F. Li, W. C. Yoo, M. B. Beernink, and A. Stein, "Site-Specific Functionalization of Anisotropic Nanoparticles: From Colloidal Atoms to Colloidal Molecules," *J. Am. Chem. Soc.*, **131** [51] 18548-55 (2009).
21. F. Li, Z. Wang, N. S. Ergang, C. A. Fyfe, and A. Stein, "Controlling the Shape and Alignment of Mesopores by Confinement in Colloidal Crystals: Designer Pathways to Silica Monoliths with Hierarchical Porosity," *Langmuir*, **23** [7] 3996-4004 (2007).
22. A. Stein, "Advances in Microporous and Mesoporous Solids: Highlights of Recent Progress," *Adv. Mater.*, **15** [10] 763-75 (2003).
23. H. Yan, C. F. Blanford, W. H. Smyrl, and A. Stein, "Preparation and Structure of 3D Ordered Macroporous Alloys by PMMA Colloidal Crystal Templating," *Chem. Commun.*, **2000** [16] 1477-78 (2000).
24. J. C. Lytle and A. Stein, "Recent Progress in Synthesis and Application of Inverse Opals and Related Macroporous Materials Prepared by Colloidal Crystal Templating," pp.1-79 in Annual Reviews of Nano Research, Vol. 1, Ed. by G. Cao and C. J. Brinker, World Scientific Publishing Co., 2006.
25. C. F. Blanford, R. C. Schroden, M. Al-Daous, and A. Stein, "Tuning Solvent-Dependent Color Changes of Three-Dimensionally Ordered Macroporous (3DOM) Materials through Compositional and Geometric Modifications," *Adv. Mater.*, **13** [1] 26-9 (2000).
26. C. F. Blanford, H. Yan, R. C. Schroden, M. Al-Daous, and A. Stein, "Gems of Chemistry and Physics: Three-Dimensionally Ordered Macroporous (3DOM) Metal Oxides," *Adv. Mater.*, **13** [6] 401-7 (2001).
27. R. C. Schroden, M. Al-Daous, C. F. Blanford, and A. Stein, "Optical Properties of Inverse Opal Photonic Crystals," *Chem. Mater.*, **14** [8] 3305-15 (2002).
28. A. Stein, F. Li, and N. R. Denny, "Morphological Control in Colloidal Crystal Templating of Inverse Opals, Hierarchical Structures, and Shaped Particles," *Chem. Mater.*, **20** [3] 649-66 (2008).
29. C. I. Aguirre, E. Reguera, and A. Stein, "Tunable Colors in Opals and Inverse Opal Photonic Crystals," *J. Adv. Funct. Mater.* **20** [8] 2565-78 (2010).
30. L. Vechot, J. E. H. Buston, J. Kay, G. A. Round, S. Masharani, G. A. Tickle, and R. Rowlands, "Experimental Study of the Liquid Phase Hydrolysis Reaction in Titanium Tetrachloride"; pp. 238-45 in *Proceedings of the Hazards XXII conference. Inst. Chem. Eng.*, 2011.
31. Y. Chen, A. Lin, F. Gan, "Preparation of nano-TiO₂ from TiCl₄ by Dialysis Hydrolysis," *Powder Technol.*, **167** [3] 109-16 (2006).